Oxidation of organic diselenides and ditellurides by H_2O_2 for bioinspired catalyst design

Bortoli, Marco; Zaccaria, Francesco; Tiezza, Marco Dalla; Bruschi, Matteo; Guerra, Célia Fonseca; Bickelhaupt, F. Matthias; Orian, Laura

published in
Physical Chemistry Chemical Physics
2018

DOI (link to publisher)
10.1039/c8cp02748j

document version
Publisher's PDF, also known as Version of record

PCCP

PAPER

View Article Online
View Journal | View Issue

Cite this: *Phys. Chem. Chem. Phys.*, 2018, **20**, 20874

Oxidation of organic diselenides and ditellurides by H_2O_2 for bioinspired catalyst design†

Marco Bortoli, [a] Francesco Zaccaria, [b] Marco Dalla Tiezza, [a] Matteo Bruschi, [a] Célia Fonseca Guerra, [bc] F. Matthias Bickelhaupt *[bd] and Laura Orian *[a]

Received 1st May 2018,
Accepted 24th July 2018

DOI: 10.1039/c8cp02748j

rsc.li/pccp

The reactivity of diselenides and ditellurides of general formula $(RX)_2$ (X = Se, Te; R = H, CH_3, Ph) toward hydrogen peroxide was studied through a computational approach based on accurate Density Functional Theory (DFT) calculations. The aliphatic and aromatic dichalcogenides have been chosen in light of their activity in glutathione peroxidase (GPx)-like catalytic cycles and their promising features as efficient antioxidant compounds. The reaction products, the energetics and the mechanistic details of these oxidations are discussed. Analogous disulfides are included in our analysis for completeness. We find that the barrier for oxidation of dichalcogenides decreases from disulfides to diselenides to ditellurides. On the other hand, variation of the substituents at the chalcogen nucleus has relatively little effect on the reactivity.

1 Introduction

In 1817, J. J. Berzelius identified by serendipity a new element, selenium,[1] in the process of making sulfuric acid. The first recognized role of selenium in biology was as a toxin, firstly studied in livestock diseases,[2] and only twenty years later it was discovered that it is an essential element to bacteria,[3] and animals.[4,5] Only in the late 1970s, the presence of selenium was found in the so-called "21st amino acid",[6] selenocysteine (Sec). Sec accounts for most of the selenium in the human body, being incorporated into 25 proteins.[7–9] Among these, glutathione peroxidases (GPxs) have attracted continuing interest, after Sec was discovered in their catalytic pocket.[10,11] These enzymes are ubiquitous in all kingdoms of life and catalyze the reduction of H_2O_2 and organic hydroperoxides, using glutathione (GSH) as cofactor. Among other functions, they have the important role of controlling the oxidative stress inside the cell, which results from the formation of reactive oxygen species (ROS) like H_2O_2 and hydroperoxides. If not strictly controlled, the oxidative stress can lead to cell damage and to a variety of degenerative processes, including inflammation, cardiovascular pathologies, dementia and cancer, and death.

Notably, Sec plays a crucial role in the GPx enzymatic cycle. In fact, a significant drop of catalytic activity occurs when the Sec residue is mutated into the more common cysteine (Cys).[12,13] The GPx function was experimentally confirmed in different occasions[14,15] as well as assessed *in silico*.[16–18] It is consolidated that the first mechanistic step involves the oxidation of Sec by H_2O_2 or ROOH to a selenenic acid form and leads to the formation of water or alcohol, respectively (see ESI,† Scheme S1, oxidative phase). The details of this reaction occurring in the GPx active site as well and in the active sites of the S and Te GPx mutants, have been reported very recently in a combined classic and quantum mechanics study,[19] which establishes that the presence of selenium is neatly energetically advantageous also in this stage. In fact, the peculiar biological role of selenium is still under debate, despite, as can be gathered from our initial historical excursus, more than 200 years have passed since its discovery.

The study of key-elementary biological reactions involving chalcogen centers is fundamental and can provide hints for the design of efficient anti-oxidant GPx like molecular mimics and of active Se-based catalysts for organic chemistry. Among the numerous organoselenides, which have been synthesized and tested as potential anti-oxidant drugs *in vivo* as well as *in vitro* in the last three decades,[20–22] diaryldiselenides are considered of great importance. Since the discovery that diaryldiselenides can prevent liver necrosis in vitamin E deficient rats,[23] this class of compounds became the focus of intensive research to assess their possible biological and pharmacological use. For an extensive review on the subject the reader can refer to a

[a] *Dipartimento di Scienze Chimiche, Università degli Studi di Padova, Via Marzolo 1, 35131 Padova, Italy. E-mail: laura.orian@unipd.it*
[b] *Department of Theoretical Chemistry and Amsterdam Center for Multiscale Modeling (ACMM), Vrije Universiteit Amsterdam, De Boelelaan 1083, 1081 HV Amsterdam, The Netherlands. E-mail: f.m.bickelhaupt@vu.nl*
[c] *Leiden Institute of Chemistry, Leiden University, PO Box 9502, 2300 RA Leiden, The Netherlands*
[d] *Institute for Molecules and Materials (IMM), Radboud University, Heyendaalseweg 135, 6525 AJ Nijmegen, The Netherlands*

† Electronic supplementary information (ESI) available. See DOI: 10.1039/c8cp02748j

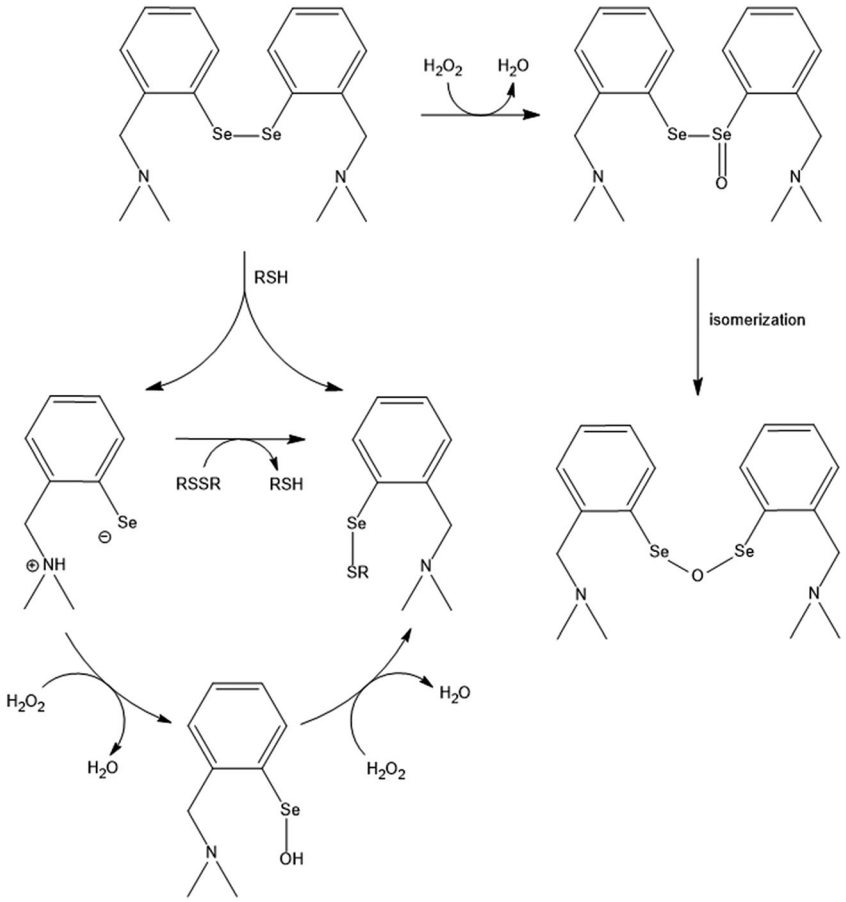

Scheme 1 Oxidation of 2-(*N*,*N*-(dimethylamino)-methyl)benzenediselenide by H_2O_2 followed by product isomerization to anhydride; the reaction mechanism with a thiol (RSH), which is energetically favored, is also shown.

review and a recent paper by Rocha *et al.*[22,24] These mimics are particularly promising because two Se nuclei are present and the chalcogen–chalcogen bond may be weakened and even broken upon oxidation or reduction, leading to the formation of two separated catalytic centers. Theoretical mechanistic studies on their reactivity are fragmentary, as discussed in two recent reviews.[25,26] Studies on the reactivity of an analogue of diphenyl diselenide,[27] show evidence that the first step in the GPx-like mechanism is the reaction with a thiol resulting in the reduction of one selenium to selenol with the concomitant cleavage of the selenium–selenium bond and formation of a selenenyl sulfide (Scheme 1); in this particular case, the presence of the *ortho* amino group stabilizes the zwitterionic form of the selenol. The direct reaction of the same compound with H_2O_2 (Scheme 1) was also studied *in silico*,[28] but was found to be disfavored: it resulted in the formation of a selenolseleninate with a strongly distorted structure, leading the authors to exclude the feasibility of this pathway. Moreover, there is still a debate on the product of this direct oxidation by H_2O_2: experimental studies on ebselen‡ [29–31] suggest that the reaction of its diselenide intermediate, obtained by dimerization, with H_2O_2 leads to the formation of a selenenic anhydride,[32,33] although no evidence is provided. Conversely, computational studies[34,35] propose the initial formation of a selenolseleninate. The formation of the anhydride would then be possible upon subsequent isomerization.

The reason why selenium has not been substituted by sulfur along the evolution path is another puzzling aspect related to the presence of Sec in human proteins. In fact, Sec insertion mechanism is much more complicated than that of simple Cys.[36,37] Therefore, Sec must provide a clear advantage over the more common sulfur based amino acid. Traditionally, the lower pK_a of Sec compared to that of Cys (5.2 *vs.* 8.3),[38] and its better leaving group and electron acceptor ability were regarded as the main reasons for which selenium was preferred over sulfur.[39] However, studies on *Drosophila melanogaster* have shown that, in some complex eukaryotes, no significant loss of activity is found when Sec is substituted by Cys.[40] This has contributed to shift the current opinion on the reason why selenium is still present in biology toward the view that it is its ability to be oxidized and then readily reduced in a reversible way that makes selenium more advantageous than sulfur.[39,41,42] Thus, systematic studies on organoselenides and their redox properties are important for future application of these compounds. These perspectives

‡ Ebselen (2-phenyl-1,2-benzisoselenazol-3(2*H*)-one)[29,30] is the best known GPx mimic, but its catalytic activity toward different peroxides is orders of magnitude lower than that of the enzyme.[31]

go beyond pharmaceutical synthesis and drug design, because organoselenides are widely used also in organic synthesis. For example, it is well known that the oxidation of organoselenides by H_2O_2 to selenoxides leads to easy elimination with formation of alkenes when β hydrogens are present. Another example is the catalytic role of organoselenides in organic oxidations, since upon oxidation by H_2O_2 a perseleninic agent forms, which is a powerful oxidant. These aspects and the reaction mechanisms have been recently reported by some of us.[43]

If selenium has been preferred to sulfur by nature in selected cases, no biological role has been proved for tellurium yet. Nevertheless, recent experiment on semisynthetic telluroproteins,[44,45] revealed that a high peroxidase activity is achieved when the Sec residue is substituted with tellurocysteine (Tec). In the last two decades, researchers have been evaluating a possible use of organotellurium compounds in pharmacology.[24,46] Studies on the topic are still in their infancy and, although in most instances the activity of organotellurides compounds was found comparable if not superior to that of their selenium analogues, their toxicity *in vivo* has yet to be fully assessed. Therefore, caution is needed when evaluating them for therapeutic use because their potential pro-oxidant effects could completely outweigh their beneficial activity.[21,47]

All the arguments expressed so far draw a clear picture of the possible uses of organodiselenides and organoditellurides as antioxidant in pharmacology and therapy, while the use of organodiselenides in organic synthesis is abundantly diffuse. There are still uncertainties though regarding the understanding of the behavior of these molecules in their catalytic activity because, to the best of our knowledge, scarce systematic mechanistic studies have been carried out on these compounds. To this purpose, state-of-the-art computational methodologies provide a useful approach to analyze their reactivity in the presence of an oxidizing agent. Quantum mechanical DFT methodologies have been proven to be reliable and effective in describing the energetics of organochalcogen compounds,[48] resulting in the method of choice for many studies on these systems.[16,18,49,50] In this work, we aim at providing an exhaustive *in silico* description of the oxidation of model diselenides and ditellurides by H_2O_2. Moreover, since the understanding of the different properties of the chalcogens at a more fundamental level could give precious insight on how to fine tune their reactivity, a comparison with sulfur analogues will be presented in a few selected cases.

2 Computational methodology

The reaction of H_2O_2 with nine different diselenides and ditellurides of general formula RXXR has been investigated *in silico*; the structures and the naming scheme of the chosen compounds can be seen in Scheme 2. For the simplest compounds (*i.e.* those with R = H, CH_3 and Ph) the sulfur variants were also investigated for completeness.

All DFT calculations were carried out with the Amsterdam Density Functional (ADF) modeling suite.[51–54] Relativistic effects

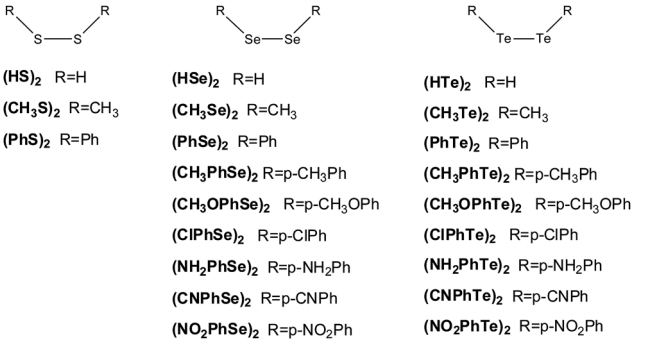

Scheme 2 Structure and naming scheme of the studied diselenides and ditellurides.

were included in the calculations using the scalar relativistic zeroth-order regular approximation (ZORA).[55] The OLYP[56–59] functional was employed in conjunction with the TZ2P basis set, which is a large and uncontracted set of Slater-type orbitals (STOs) of triple-ζ quality, augmented with two sets of polarizations functions for each atom: 2p and 3d for hydrogen, 3d and 4f in the case of carbon, nitrogen, oxygen and chlorine, 4d and 4f for selenium and 5d and 4f for tellurium. The frozen core approximation was employed: up to 1s for carbon, nitrogen and oxygen, up to 2p for chlorine, up to 3p for selenium and up to 4p for tellurium. We will refer to this level of theory as ZORA-OLYP/TZ2P.

For a selected number of cases, dispersion corrections were added to the calculation. In these computations, the BLYP[57–60] functional in combination with the TZ2P basis set was employed. Dispersion corrections were taken into account with the D3 scheme with inclusion of the Becke Johnson damping (D3(BJ)), developed by Grimme *et al.*[61] This level of theory is denoted ZORA-BLYP-D3(BJ)/TZ2P. The performance of DFT methods in describing nucleophilic susbtitutions involving organochalcogen compounds has been assessed in earlier benchmark studies including HF, MP2 and MP4 methods.[62–66] In presence of phenyl groups, there is also the possibility of π-stacking and other weak interactions that critically depend on dispersion forces, but more recent extensive benchmarks show that DFT with Grimme's D3-dispersion correction performs very well as compared to highly correlated *ab initio* methods such as CCSD(T).[67,68]

Stationary points were fully optimized and frequency calculations were used to verify the results. For all energy minima, only real frequencies associated with the vibrational normal modes were found. In the case of the transition states, only one imaginary frequency resulted from the computation, corresponding to the normal mode associated with the reaction under investigation.

To obtain a better picture regarding the contributions that account for the differences in the energy barriers, activation strain analyses (ASAs) were carried out. The activation strain model, also known as distortion/interaction model,[69] is a fragment-based method in which the height of a reaction barrier is described in terms of properties of the reactants involved. In our case, the fragments are the dichalcogenide substrate and H_2O_2.

In this scheme, the total bonding energy (ΔE) is decomposed into two contributions (eqn (1)):[70–72]

$$\Delta E = \Delta E_{\text{strain}} + \Delta E_{\text{int}} \quad (1)$$

The two terms on the right-hand side of eqn (1) are respectively the energy needed to deform the fragments from their initial geometry to the one they acquire in the reactant complex and in the transition state (ΔE_{strain}) and the actual interaction energy between the two deformed fragments (ΔE_{int}). This latter term can be further decomposed, in the framework of Kohn–Sham molecular orbital theory, into electrostatic attraction (ΔV_{elst}) between the unperturbed fragments, Pauli repulsion (ΔE_{Pauli}, that is the repulsive interaction between occupied orbitals) and orbital interaction (ΔE_{oi}) using a quantitative energy decomposition analysis (EDA, eqn (2)):[73]

$$\Delta E_{\text{int}} = \Delta V_{\text{elst}} + \Delta E_{\text{Pauli}} + \Delta E_{\text{oi}} \quad (2)$$

In the case of the smaller compounds (*i.e.* **(HX)$_2$**, **(CH$_3$X)$_2$** and **(PhX)$_2$**), for the oxidation reaction, we performed ASA along the reaction coordinate (ζ) from the reactant complex **RCox** until **TSox** to evaluate the different contributions to the activation barrier. In fact, the eqn (1) and (2) can be written for all points along a defined reaction coordinate and become:

$$\Delta E(\zeta) = \Delta E_{\text{strain}}(\zeta) + \Delta E_{\text{int}}(\zeta) \quad (3)$$

$$\Delta E_{\text{int}}(\zeta) = \Delta V_{\text{elst}}(\zeta) + \Delta E_{\text{Pauli}}(\zeta) + \Delta E_{\text{oi}}(\zeta) \quad (4)$$

All the geometries of the non-stationary points, employed in ASA end EDA calculations, were obtained from an intrinsic reaction coordinate (IRC) computation, starting from the transition state following the path along the normal mode associated with the negative frequency with a steepest descent algorithm. ASA and EDA values were then calculated from the IRC geometries using the program PyFrag.[74]

For the remaining compounds, we restricted the analysis only to the stationary points (*i.e.* **RCox** and **TSox**).

3 Results and discussion

The oxidation of model dichalcogenides (Scheme 2) was investigated at the ZORA-OLYP/TZ2P level of theory, according to the reaction depicted in Scheme 3; subsequently the redox isomerization to anhydride was also considered.

3.1 Oxidation of diselenides and ditellurides by H_2O_2

First, we focus our analysis on the oxidation of the smaller compounds (*i.e.* **(HX)$_2$**, **(CH$_3$X)$_2$** and **(PhX)$_2$**). In agreement with recent papers by some of us,[48,75] the optimized starting structures for these compounds were found to be very similar and show a ψ dihedral angle (Fig. 1) in the range from 91° for **(HSe)$_2$** to 83° in the case of **(PhTe)$_2$**, in line with the bonding mechanism established previously for dichalcogenides.[76,77] Importantly, it has been demonstrated[48] that variations of ψ are energetically meaningful, while variation of ϕ are negligible. To this purpose, numerous functionals perform quite similarly and rather well in reproducing the skewed arrangement of the groups linked to the chalcogens, the energy associated to their rotation and OLYP reproduces the correct trend for the chalcogen–chalcogen homolytic dissociation. Notably, the inclusion of dispersion correction for selected GGA functionals leads to a stabilization of the conformation with ψ equal to zero and stacked phenyls in diphenyldiselenides and diphenylditellurides, a conformation which in any case never becomes a minimum: skewed conformations, *i.e.* with phenyls at approximately 90 degrees, are the most stable structures, for the description of which the inclusion of dispersion is not crucial.

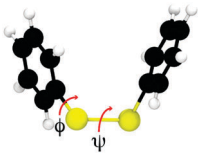

Fig. 1 **(PhSe)$_2$** optimized structure; ψ and ϕ dihedral angles are shown.

The first oxidation step proceeds with the formation of a reactant complex (**RCox**) which is slightly more stable than the free reactants (Table 1) through a transition state (**TSox**) in which the O–O bond in H_2O_2 is elongated, shifting one of the oxygen atoms towards one of the S/Se/Te centers, and the ψ dihedral angle ranges from 161° to 168° conferring the structures a "*trans*-like" geometry if the inter chalcogen bond is considered; the case of **(PhSe)$_2$** is shown in Fig. 2 as example. The resulting product complexes (**PCox**) maintain almost identical ψ values with a chalcogen–oxygen bond length of 1.49 Å in the case of sulfur, 1.65 Å in the case of selenium and 1.82 Å in the case of tellurium, with a variation of no more than 0.01 Å among the different structures, for all the three chalcogens. In all cases, the product complex is stabilized with respect to the initial reactant complex. A different pathway was also investigated in the case of the phenyl substituted compounds, in which both **TSox** and **PCox** maintain a ψ dihedral smaller than 90° throughout the oxidation reaction, but the energies of the new transition states were found to differ from the previous ones by amounts lower than chemical accuracy (see Table S1, ESI†); therefore, this alternative pathway was not considered in our analysis.

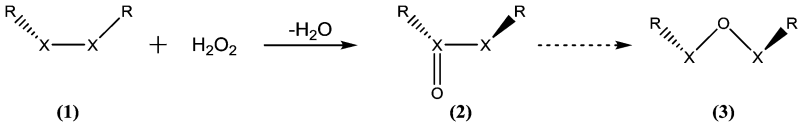

Scheme 3 Reaction mechanism for the direct oxidation and subsequent possible redox isomerization of diphenyl diselenides and ditellurides; the definitions of R and X are given in Scheme 2.

Table 1 Relative energies (kcal mol^{-1}) of stationary points for the oxidation of RXXR (X = S, Se, Te; R = H, CH_3, Ph) by H_2O_2; level of theory: ZORA-OLYP/TZ2P

		R			
X		H		CH_3	Ph
S	**RCox**	−0.5	(−4.4)[a]	−1.7	−1.7
	TSox	25.2	(16.5)	23.8	24.1
	PCox	−48.4	(−49.7)	−53.4	−52.9
Se	**RCox**	−1.5	(−5.9)	−2.7	−2.0
	TSox	20.2	(10.3)	17.5	19.1
	PCox	−36.1	(−40.2)	−42.3	−42.4
Te	**RCox**	−1.5	(−5.4)	−2.3	−1.9
	TSox	14.0	(4.0)	12.4	12.4
	PCox	−38.5	(−43.9)	−43.1	−44.7

[a] Values in parenthesis are computed at ZORA-BLYP-D3(BJ)/TZ2P level of theory.

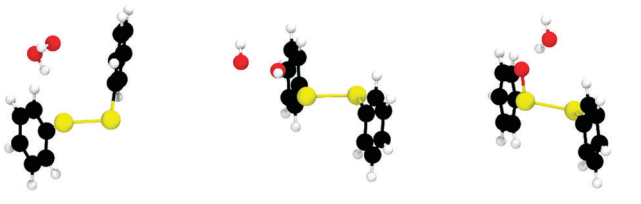

Fig. 2 Reactant complex **(RCox)**, transition state **(TSox)** and product complex **(PCox)** structures for the oxidation of **$(PhSe)_2$**.

Reactant complexes are only weakly bound, going from −0.5 kcal mol^{-1} in the case of **$(HS)_2$** to −2.7 kcal mol^{-1} for **$(CH_3Se)_2$**, and are computed to be within about one kcal mol^{-1} among the various dichalcogenides (Table 1). Differences become larger when we consider transition states and product complexes. Thus, reaction barriers are the lowest for tellurium compounds and pronouncedly increase when going from Te to Se and S compounds. This effectively makes the ditellurides the easiest to oxidize. Reaction energies show an opposite trend: they are most exothermic for sulfur compounds and become less so for selenium and tellurium compounds, the latter two differ only slightly.

Shifting the focus on the effect of the R substituent, only slight differences are computed when going from **$(HX)_2$** to **$(CH_3X)_2$** and finally to **$(PhX)_2$**. **$(HX)_2$** compounds show the least stabilized reactant complexes, but the highest difference between two structures is of 1.2 kcal mol^{-1}. R substituent effect is found to be very small also on activation energies which all fall in a 1.5 kcal mol^{-1} range, stressing once more the fact that the three substituents R = H, CH_3, Ph have not a strong impact on the reaction energetics. On the other hand, a significant difference between **$(HX)_2$** and **$(CH_3X)_2$** is found in the **PCox**s, as the latter are more stable in energy by approximately 5 kcal mol^{-1}. Looking at **$(PhX)_2$** energies, they are very similar to those of **$(CH_3X)_2$**. Moreover, this difference goes in favor of the methyl substituted molecule in the case of disulfides, whereas, in the case of ditellurides, the phenyl substituted **PCox** is found to be the most stable.

3.2 Activation strain analysis for the oxidation of RXXR (R = H, CH_3, Ph) by H_2O_2.

The description of the energetics of these reactions is certainly not enough to assess the different behavior as the chalcogen or the substituents are modified. Therefore, the activation strain model combined with a quantitative energy decomposition analysis was employed to study the oxidations along the reaction path. Since the main goal of this investigation was to elucidate the nature of the different energy barriers, ASA end EDA were applied from **RCox** to **TSox**. The oxygen–oxygen distance in H_2O_2 is a critical geometry parameter: it defines the progress of the reaction regardless of the chalcogen atom involved, and was therefore selected as a suitable reaction coordinate, along which the activation strain and energy decomposition were subsequently calculated. The system was partitioned into two fragments, *i.e.*, the dichalcogenide and H_2O_2. Starting from **TSox**, IRC calculations were performed to the **RCox** and ASA was carried out at each IRC point. The resulting curves are shown in the activation strain diagrams in Fig. 3 and 4. Moreover, at the **RCox** and **TSox** points the interaction energy was further decomposed into the three contributions stemming from electrostatic interactions (ΔV_{elst}), orbital interactions (ΔE_{oi}) and Pauli repulsion (ΔE_{Pauli}) (Table S2, ESI†).

3.3 Effect of the chalcogen

Firstly, we discuss the chalcogen effect. In the simplest set of compounds, *i.e.* **$(HX)_2$**, we have investigated the effect of the inclusion of dispersion, performing calculations also at ZORA-BLYP-D3(BJ)/TZ2P level of theory (Table 1), as benchmarked.[48,75] This results in lowering of the energies of **RCox** by approximately 5 kcal mol^{-1} and lowering of the activation energies by the same amount of energy. In addition, also the reaction energies become more negative by approximately 5 kcal mol^{-1}, except in the case of the disulfide where no appreciable variation is found. This indicates that the inclusion of dispersion makes the oxidation energetically more favored, but the trend is nicely maintained with almost constant energy shift. In Fig. 3, the role of dispersion correction can be inspected also along the reaction coordinate.

Looking at the curves in Fig. 3 (left) and Fig. 4 (left), for the hydrogen and methyl substituted dichalcogenides, it is clear that, throughout all the reaction, the strain energy profiles are almost identical. This is a strong indication that, in this case, most of this contribution comes from the deformation of the O–O bond. Phenyl substituted structures (Fig. 4 right) display a more complex behavior since ΔE_{strain} profile is clearly different for the three reactions. In particular, at the early stages of the reaction strain is very similar among the three chalcogens, but, as the oxidation proceeds, the three curves increase at different rates. **$(PhSe)_2$** is the structure that has the highest strain followed by **$(PhS)_2$** and **$(PhTe)_2$**.

Interestingly, ΔE_{int} curves do not show a monotonous decrease (*i.e.* strengthening in stabilization) along the reaction coordinate, but there is a window inside which they increase, leading to positive (that is destabilizing) interaction energy values.

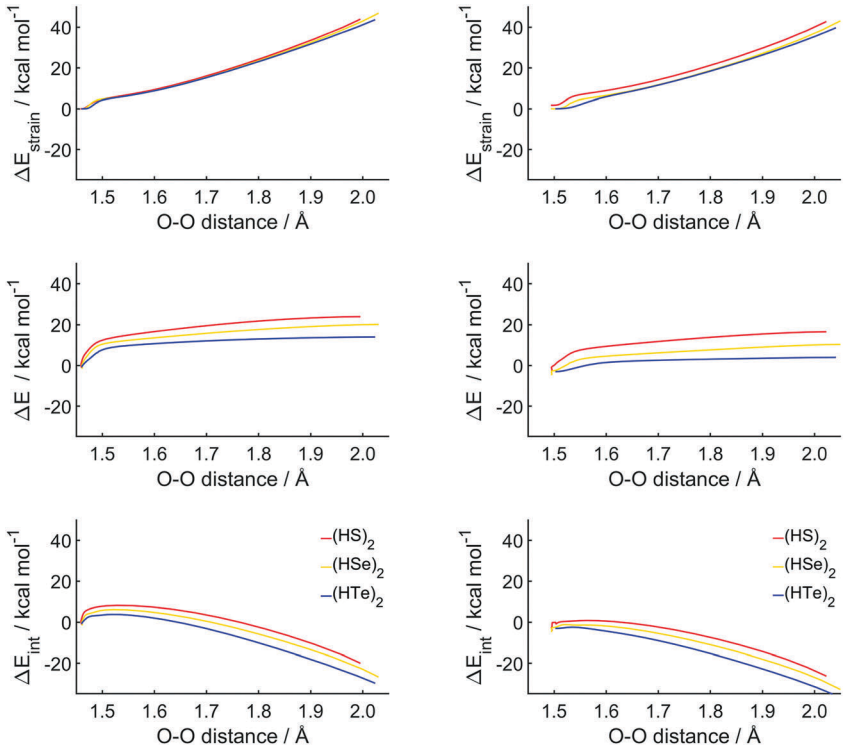

Fig. 3 Activation strain analysis along the reaction path for the oxidation of **$(HX)_2$**, without (left) and with (right) empirical correction for dispersion. Pure electronic energies are relative to the free reactants; level of theory: ZORA-OLYP/TZ2P (left) and ZORA-BLYP-D3(BJ)/TZ2P (right).

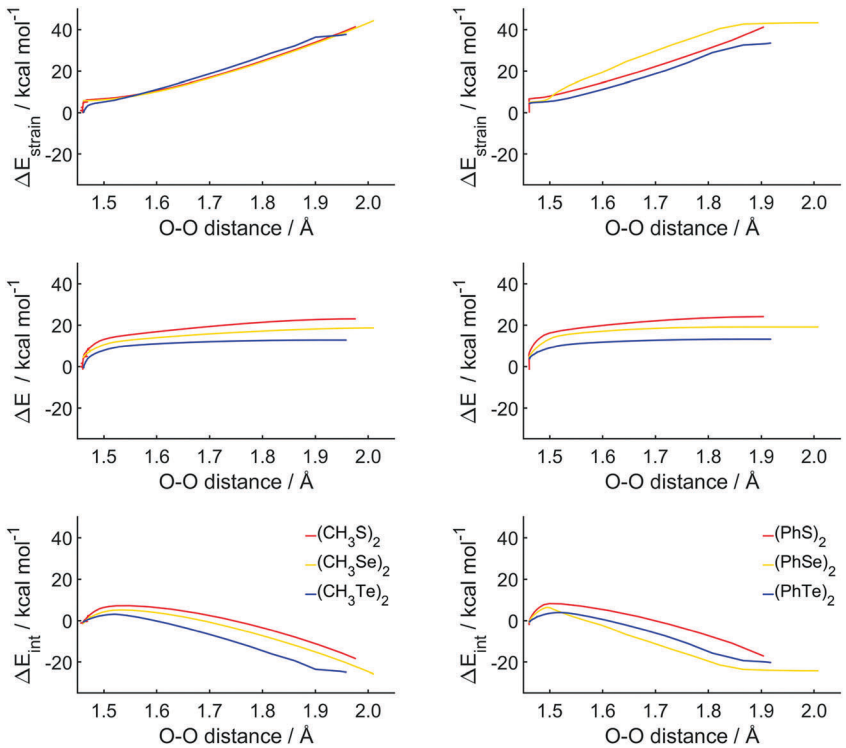

Fig. 4 Activation strain analysis along the reaction path for the oxidation of **$(CH_3X)_2$** (left) and **$(PhX)_2$** (right). Pure electronic energies are relative to the free reactants; level of theory: ZORA-OLYP/TZ2P.

This destabilizing interaction, found for all the nine cases of Fig. 3 (left) and Fig. 4, is due to an initial rotation of the H_2O_2 molecule. In this way, the H-bond found in **RCox**, formed by the chalcogen atom and a proton of H_2O_2 (see Fig. 2), is broken

and an oxygen atom is found directly pointing towards the chalcogen. This situation of two electron rich atoms (the chalcogen and the oxygen) pointing toward each other is, initially, not favorable, due to high Pauli repulsion and it is the reason why ΔE_{int} is computed to be positive until the two fragments reach a distance and orientation at which stabilizing orbital overlap becomes relevant, making ΔE_{oi} dominant and the overall interaction negative (*i.e.* stabilizing) again. Moreover, computed energies for the frontier orbitals of the different dichalcogenides showed that the HOMO energy decreases going from the least electronegative atom (Te) to the most electronegative one (S). This clearly translates to a more favorable interaction energy in the cases of the selenium and tellurium compounds, both the hydrogen- and methyl-substituted ones, due to the better energy match with the LUMO of H_2O_2. In the case of phenyl containing complexes the situation is again different with an initial stage analogous to that of H and CH_3 substituted structures, followed by an inversion which results in **$(PhSe)_2$** showing the most favorable ΔE_{int} for most of the reaction.

However, the total ΔE profiles show the same trend in all cases, that is tellurium compounds have the lowest oxidation barriers followed by selenium and then sulfur ones.

3.4 Effect of the substituent

When analyzing the effect of the substituent, it must be immediately stressed that it is much weaker than that of the chalcogen. Looking at the data in Table 1, it is clear that stationary points of methyl and phenyl substituted compounds display very close energies (which differ by less than 1 kcal mol^{-1}), whereas in hydrogen substituted species slightly larger differences are found. These latter compounds show less stabilized **RCox**s and **TSox**s, effectively making them the most difficult to oxidize. Methyl and phenyl dichalcogenides have smaller oxidation barriers, although the largest difference with the HXXH is of 1.5 kcal mol^{-1} in the case of **$(CH_3Se)_2$**.

To further investigate if an electronic perturbation on the rings may have a substantial effect on the magnitude of the activation energies, the oxidation of diphenyldichalcogenides with *para* substituents was modeled. Since the focus of this work is on the different properties of diselenides and ditellurides as efficient antioxidants, sulfur compounds were not included in this study of aromatic substituted dichalcogenides.

The optimized structures for diselenides and ditellurides have a ϕ angle close to 90°, with the phenyl rings lying in almost parallel planes, giving the compounds an "open" conformation, if we compare the aromatic rings to saloon doors (Fig. 5, right).[48,75] The only exceptions were found to be **$(CNPhSe)_2$** and **$(NO_2X)_2$** in which this dihedral is close to 0° and gives the molecule a "closed" conformation (Fig. 5, left). Mechanistically, they behave exactly like the hydrogen and methyl substituted dichalcogenides, presenting structures very similar to those of Fig. 2. Computed energies show that the oxidation barrier increases going from **$(NH_2PhSe)_2$** to **$(NO_2PhSe)_2$**. The former requires an activation energy of 20.3 kcal mol^{-1}, whereas 24.1 kcal mol^{-1} are needed for the latter. In between these two extreme values, all the other substituted compounds are

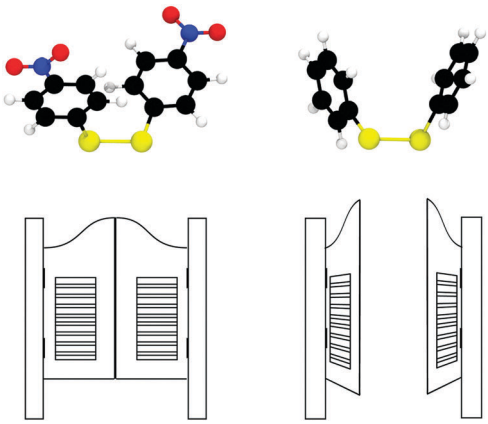

Fig. 5 Examples of the "closed" (left) and "open" (right) structures found in aryl dichalcogenides.

positioned (Table 2). The series follows the electron donor character of the moiety attached to the phenyl ring with a barrier that increases in the order $NH_2 < CH_3O < CH_3 < Cl < CN < NO_2$. The resulting **PCox**s are largely stabilized (computed relative energies are around −40 kcal mol^{-1}), making the process energetically favored. Moving to tellurium derivatives, a similar trend is found in all cases, both for **TSox** and **PCox**, but with energy barriers lower than those of selenium by approximately 5 kcal mol^{-1}. The overall effect of the *para* group bonded to the phenyl rings is quite small, resulting in a difference between the highest and the lowest barrier of 3.8 kcal mol^{-1}, in the case of diselenides, and of 2.1 kcal mol^{-1} in the case of ditellurides, respectively. The fact that this trend in activation energy correlates well with the electron donor character of the *para* substituents of the ring (the NH_2 and CN groups, which have the lowest and highest activation energy, are the strongest electron donating and strongest electron withdrawing groups, respectively), is a robust evidence that in this kind of reaction the chalcogen acts as nucleophile, since an increased electron density in its proximity facilitates the reaction.

The activation strain analysis was applied to **RCox**s and **TSox**s and shows a different behavior for the two chalcogens. For the diselenides, the increase in the oxidation barrier is mainly due ΔE_{strain} in **TSox** (Table 3) which increases from 41.3 kcal mol^{-1} in the case of **$(NH_2PhSe)_2$** to 46.7 kcal mol^{-1} in the case of **$(NO_2Se)_2$**. For the same structures, ΔE_{int} increases only by 0.5 kcal mol^{-1}.

Table 2 Relative energies (kcal mol^{-1}) of the stationary points for the oxidation of substituted diselenides and ditellurides by H_2O_2; level of theory: ZORA-OLYP/TZ2P

		R					
X		CH_3Ph	CH_3OPh	ClPh	NH_2Ph	CNPh	NO_2Ph
Se	**RCox**	−2.9	−2.2	−1.8	−2.7	−1.0	−1.6
	TSox	17.8	18.1	19.9	17.6	21.7	22.5
	PCox	−43.4	−43.1	−41.9	−43.4	−40.6	−39.7
Te	**RCox**	−2.1	−2.8	−1.7	−2.5	−1.5	−0.6
	TSox	12.8	12.5	13.9	11.9	15.0	15.9
	PCox	−44.9	−45.5	−44.2	−45.6	−43.5	−42.5

Table 3 Relative energies and activation strain analysis (in gas phase in kcal mol^{-1}) for the first oxidation of substituted diphenyldiselenides and diphenylditellurides by H_2O_2; level of theory: ZORA-OLYP/TZ2P

		Se				Te			
R		ΔE_{strain}	ΔE_{int}	ΔE	$\Delta E^{\ddagger}$	ΔE_{strain}	ΔE_{int}	ΔE	$\Delta E^{\ddagger}$
NH_2	**RCox**	0.1	−2.8	−2.7		0.1	−2.6	−2.5	
	TSox	41.3	−23.7	17.6	20.4	32.3	−20.4	11.9	14.4
CH_3O	**RCox**	0.1	−2.3	−2.2		0.2	−3.0	−2.8	
	TSox	41.9	−23.8	18.1	20.3	30.5	−18.0	12.5	15.3
CH_3Ph	**RCox**	−0.7	−2.2	−2.9		0.1	−2.2	−2.1	
	TSox	42.0	−24.2	17.8	20.7	31.4	−18.4	12.8	14.9
Cl	**RCox**	0.1	−1.9	−1.8		0.1	−1.8	−1.7	
	TSox	44.0	−24.1	19.9	21.7	36.5	−22.6	13.9	15.6
CN	**RCox**	0.5	−1.5	−1.0		0.1	−1.6	−1.5	
	TSox	45.9	−24.2	21.7	22.7	40.2	−25.2	15.0	16.5
NO_2	**RCox**	0.3	−1.9	−1.6		0.9	−1.3	−0.6	
	TSox	46.7	−24.2	22.5	24.1	41.7	−25.8	15.9	16.5

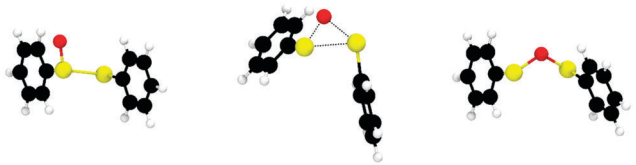

Fig. 6 Stationary points and transition state structures for the isomerization of **$(PhSe)_2$**.

Moreover, the starting reactant complexes show a slight decrease in stabilization, when going from **$(NH_2PhSe)_2$** to **$(NO_2PhSe)_2$**, but this is not sufficient to balance the increased **TSox** energy, resulting in overall higher oxidation barriers. On the other hand, for the ditellurides, ΔE_{int} of **TSox** increases, when going from **$(NH_2PhTe)_2$** to **$(NO_2PhTe)_2$**, by 5.4 kcal mol^{-1}, but this is accompanied by a much larger increase in ΔE_{strain} (9.4 kcal mol^{-1} between the two extreme compounds) and this leads to an overall higher reaction barrier. The reactant complexes show a loss of stabilization, in presence of weaker electron donating substituents, due to a decrease of ΔE_{int}.

Again, molecular orbital inspection shows how HOMO energy decreases as the substituent at the *para* position becomes a stronger electron withdrawing group. This effect correlates well with the increase of the oxidation barrier as compounds with a higher HOMO present a higher reactivity towards H_2O_2.

Results from activation strain analysis for the series of substituted aromatic diselenides and ditellurides here considered confirm what found for the simpler aliphatic compounds, *i.e.* that these reactions are not much affected by the changes in electronic density around the chalcogen but, since the chalcogen atom acts as nucleophile, substituents which contribute to increase the electron density around it help to lower the required activation energy for the oxidation process through a destabilization of the HOMO of the dichalcogenide.

3.5 Redox isomerization to anhydride

Finally, the possible redox isomerization to a selenenic or tellurenic anhydride (compound (**3**) in Scheme 3) of the oxidized dichalcogenides (compound (**2**) in Scheme 3) was modeled. This reaction leads to a structure that is an intermediate in the formation of highly oxidized anhydrides which are, at least in the case of selenium, key structures in catalyzing organic reactions.[78] The water molecule formed after the first oxidation was not included in the subsequent calculations. The transition states of the intramolecular reactions were successfully optimized for all substituent–chalcogen combinations and they all exhibit similar structures. As the O–X–X angle closes, with the oxygen progressively inserting between the two chalcogen atoms, another geometrical rearrangement occurs. One of the two groups linked to the chalcogen atoms rotates by almost 90° so that the transitions state structure for the isomerization (**TSiso** in Fig. 6, depicted for **$(PhSe)_2$**) displays a dihedral angle ψ around 90°. This rotation is reversed in the second part of the reaction that leads to the formation of the selenenic or tellurenic anhydride (structure (**3**) in Fig. 6, depicted for **$(PhSe)_2$**), which again shows a dihedral angle ψ remarkably wider than 90° and an overall structure similar to that of (**2**). This process has systematically higher activation energy if compared to the initial oxidation, with computed barriers higher by more than 20 kcal mol^{-1} (Table 4). For the diselenides, they range from 41.1 kcal mol^{-1} in the case of **$(NH_2PhSe)_2$** to 45.5 kcal mol^{-1} in the case of **$(HSe)_2$** whereas for the ditellurides the range is narrower, going from 26.9 kcal mol^{-1} for **$(NO_2PhTe)_2$** to 29.5 kcal mol^{-1} of **$(HTe)_2$**. Overall, ditellurides show lower isomerization activation energies, in analogy to what found for the first oxidation. Moreover, these reactions result energetically unfavorable as

Table 4 Relative energies (with respect to **1** + H_2O_2, in kcal mol^{-1}) for the isomerization of the selenoxides and telluroxides **2**; level of theory: ZORA-OLYP/TZ2P

		R								
X		H	CH_3	Ph	CH_3Ph	CH_3OPh	ClPh	NH_2Ph	CNPh	NO_2Ph
Se	**2**	−32.6	−37.8	−38.1	−39.0	−38.5	−37.7	−38.6	−36.6	−35.8
	TSiso	12.9	6.6	4.1	3.1	3.2	4.1	2.5	4.7	5.3
	3	−23.0	−28.5	−28.7	−29.7	−29.5	−28.7	−29.9	−29.0	−29.0
Te	**2**	−34.0	−37.8	−38.6	−39.6	−39.8	−38.4	−39.9	−38.4	−37.5
	TSiso	−4.5	−9.1	−11.2	−11.3	−11.6	−11.2	−11.9	−11.4	−10.6
	3	−29.0	−32.8	−33.7	−34.0	−34.7	−33.8	−35.1	−34.4	−34.3

the anhydrides are all destabilized with respect to the initial oxides. Last, the trend established for the first oxidation reactions, which favors more electron donating substituents, is not observed in the case of the formation of the anhydride. The structures with the highest isomerization barriers are HXXH and, even among the aromatic substituted groups, the highest activation energies are computed not in presence of the most electron withdrawing substituent (*i.e.* *p*-NO_2Ph) but for $(CH_3PhX)_2$ compounds, both for diselenides and ditellurides. This is a strong indication that this process is not influenced by the electronic environment around the chalcogen center, but might be more sensitive towards steric effects, that might be present, for example in the case of the diphenyldichalcogenides, when moving the substituent closer to the chalcogen atom in *ortho* or *meta* position.

4 Conclusions

The goal of this study was to investigate the mechanistic and energetic details of the oxidation of model diselenides and ditellurides by H_2O_2. Selenium based substrates are employed as catalysts in organic synthesis. Since a few decades, these compounds are considered promising anti-oxidant GPx mimics. The interest in ditellurides is more recent with the aim of designing GPx mimics with enhanced anti-oxidant activity. We have studied *in silico* the oxidation of model dichalcogenides RXXR (X = S, Se, Te; R = H, CH_3, Ph) by H_2O_2 employing activation strain analysis along the reaction path; disulfides were added for completeness.

Our results show that when going from sulfur to tellurium the reactivity of these compounds towards H_2O_2 increases. This is mainly ascribed to the stronger interaction in the presence of the heavier chalcogens. Selenium and tellurium compounds show a higher lying HOMO which can more favorably interact with the LUMO of H_2O_2 resulting in smaller activation energies. An important result is the very similar ΔE profile obtained for dimethyl and diphenyl dichalcogenides: despite the very different nature of the R groups, the substrates react in perfectly analogous manner, suggesting that, in drug-design, the toxicity of the metabolites alone can guide the choice of the specific compound. Since diphenyldiselenides are overall less toxic than dimethyldiselenide, which has been disregarded as anti-oxidant drug, synthetic efforts and tests can focus on the former family of compounds without loss of activity.

Finally, the systematic investigation of a series of differently *para*-substituted diphenyldiselenides and ditellurides reveals that (i) the product of direct oxidation is a selenoxide/telluroxide and the energetics as well as the mechanistic details are almost unaffected by the nature of the phenyl substituent and ditellurides are in general more easily oxidized than diselenides; (ii) selenoxides/telluroxides can isomerize to the corresponding selenenic/tellurenic anhydrides. We do however find this isomerization to be endothermic (*i.e.*, anhydride formation is thermodynamically unfavorable) and associated with a high activation energy. These computational findings are in agreement with the elusiveness of these species in experiments.

Conflicts of interest

There are no conflicts to declare.

Acknowledgements

Calculations were carried out on Galileo (CINECA: Casalecchio di Reno, Italy) thanks to the ISCRA Grant STREGA (Filling the STructure–REactivity GAp: *in silico* multiscale approaches to rationalize the design of molecular catalysts.), P. I.: L. O., M. D. T. is grateful to Fondazione CARIPARO for financial support (PhD grant), C. F. G. and F. M. B. thank the Netherlands Organisation for Scientific Research (NWO) for financial support.

References

1 J. Trofast, Berzelius' Discovery of Selenium, *Chem. Int.*, 2011, **33**, 16–19.
2 K. W. Franke, A New Toxicant Occurring Naturally in Certain Samples of Plant Foodstuffs: I. Results Obtained in Preliminary Feeding Trials Eight Figures, *J. Nutr.*, 1934, **8**, 597.
3 J. Pinsent, The need for selenite and molybdate in the formation of formic dehydrogenase by members of the Coli-aerogenes group of bacteria, *Biochem. J.*, 1954, **57**, 10–16.
4 E. L. Patterson, R. Milstrey and E. L. R. Stokstad, Effect of Selenium in Preventing Exudative Diathesis in Chicks, *Exp. Biol. Med.*, 1957, **95**, 617–620.
5 K. Schwarz, J. G. Bieri, G. M. Briggs and M. L. Scott, Prevention of Exudative Diathesis in Chicks by Factor 3 and Selenium, *Exp. Biol. Med.*, 1957, **95**, 621–625.
6 J. E. Cone, R. M. Del Río, J. N. Davis and T. C. Stadtman, Chemical characterization of the selenoprotein component of clostridial glycine reductase: identification of selenocysteine as the organoselenium moiety, *Proc. Natl. Acad. Sci. U. S. A.*, 1976, **73**, 2659–2663.
7 J. F. Atkins and R. F. Gesteland, Translation: the twenty-first amino acid, *Nature*, 2000, **407**, 463–464.
8 A. Böck, K. Forchhammer, J. Heider, W. Leinfelder, G. Sawers, B. Veprek and F. Zinoni, Selenocysteine: the 21st amino acid, *Mol. Microbiol.*, 1991, **5**, 515–520.
9 G. V. Kryukov, Characterization of Mammalian Selenoproteomes, *Science*, 2003, **300**, 1439–1443.
10 J. T. Rotruck, A. L. Pope, H. E. Ganther, A. B. Swanson, D. G. Hafeman and W. G. Hoekstra, Selenium: Biochemical Role as a Component of Glutathione Peroxidase, *Science*, 1973, **179**, 588–590.
11 L. Flohé, E. A. Günzler and H. H. Schock, Glutathione peroxidase: a selenoenzyme, *FEBS Lett.*, 1973, **32**, 132–137.
12 C. Rocher, J.-L. Lalanne and J. Chaudiére, Purification and properties of a recombinant sulfur analog of murine selenium-glutathione peroxidase, *Eur. J. Biochem.*, 1992, **205**, 955–960.
13 M. Maiorino, K. D. Aumann, R. Brigelius-Flohé, D. Doria, J. van der Heuvel, J. McCarthy, A. Roveri, F. Ursini and

L. Flohé, Probing the Presumed Catalytic Triad of Selenium-Containing Peroxidases by Mutational Analysis of Phospholipid Hydroperoxide Glutathione Peroxidase (PHGPx), *Biol. Chem. Hoppe-Seyler*, 1995, **376**, 651–660.

14 R. J. Kraus, J. R. Prohaska and H. E. Ganther, *Biochim. Biophys. Acta, Enzymol.*, 1980, **615**, 19–26.

15 P. Mauri, L. Benazzi, L. Flohé, M. Maiorino, P. G. Pietta, S. Pilawa, A. Roveri and F. Ursini, *Biol. Chem.*, 2003, **384**, 575.

16 R. Prabhakar, T. Vreven, K. Morokuma and D. G. Musaev, Elucidation of the mechanism of selenoprotein glutathione peroxidase (GPx)-catalyzed hydrogen peroxide reduction by two glutathione molecules: a density functional study, *Biochemistry*, 2005, **44**, 11864–11871.

17 R. Prabhakar, T. Vreven, M. J. Frisch, K. Morokuma and D. G. Musaev, Is the protein surrounding the active site critical for hydrogen peroxide reduction by selenoprotein glutathione peroxidase? An ONIOM study, *J. Phys. Chem. B*, 2006, **110**, 13608–13613.

18 L. Orian, P. Mauri, A. Roveri, S. Toppo, L. Benazzi, V. Bosello-Travain, A. De Palma, M. Maiorino, G. Miotto, M. Zaccarin, A. Polimeno, L. Flohé and F. Ursini, Selenocysteine oxidation in glutathione peroxidase catalysis: an MS-supported quantum mechanics study, *Free Radical Biol. Med.*, 2015, **87**, 1–14.

19 M. Bortoli, M. Torsello, F. M. Bickelhaupt and L. Orian, Role of the Chalcogen (S, Se, Te) in the Oxidation Mechanism of the Glutathione Peroxidase Active Site, *ChemPhysChem*, 2017, **18**, 2990–2998.

20 K. P. Bhabak and G. Mugesh, Functional Mimics of Glutathione Peroxidase: Bioinspired Synthetic Antioxidants, *Acc. Chem. Res.*, 2010, **43**, 1408–1419.

21 M. Ibrahim, W. Hassan, D. F. Meinerz, M. dos Santos, C. V. Klimaczewski, A. M. Deobald, M. S. Costa, C. W. Nogueira, N. B. V. Barbosa and J. B. T. Rocha, Antioxidant properties of diorganoyl diselenides and ditellurides: modulation by organic aryl or naphthyl moiety, *Mol. Cell. Biochem.*, 2012, **371**, 97–104.

22 J. B. T. Rocha, B. C. Piccoli and C. S. Oliveira, Biological and chemical interest in selenium: a brief historical account, *ARKIVOC*, 2017, 457–491.

23 K. Schwarz and C. M. Foltz, Factor 3 activity of selenium compounds, *J. Biol. Chem.*, 1958, **233**, 245–251.

24 C. W. Nogueira, G. Zeni and J. B. T. Rocha, Organoselenium and organotellurium compounds: toxicology and pharmacology, *Chem. Rev.*, 2004, **104**, 6255–6285.

25 L. Orian and S. Toppo, Organochalcogen peroxidase mimetics as potential drugs: a long story of a promise still unfulfilled, *Free Radical Biol. Med.*, 2014, **66**, 65–74.

26 L. P. Wolters and L. Orian, Peroxidase activity of organic selenides: mechanistic insights from quantum chemistry, *Curr. Org. Chem.*, 2016, **20**, 189–197.

27 M. Iwaoka and S. Tomoda, A model study on the effect of an amino group on the antioxidant activity of glutathione peroxidase, *J. Am. Chem. Soc.*, 1994, **116**, 2557–2561.

28 G. S. Heverly-Coulson and R. J. Boyd, Reduction of hydrogen peroxide by glutathione peroxidase mimics: reaction mechanism and energetics, *J. Phys. Chem. A*, 2010, **114**, 1996–2000.

29 A. Wendel, M. Fausel, H. Safayhi, G. Tiegs and R. Otter, A novel biologically active seleno-organic compound. II. Activity of PZ 51 in relation to glutathione peroxidase, *Biochem. Pharmacol.*, 1984, **33**, 3241–3245.

30 A. Müller, E. Cadenas, P. Graf and H. Sies, A novel biologically active seleno-organic compound-1. Glutathione peroxidase-like activity *in vitro* and antioxidant capacity of PZ 51 (Ebselen), *Biochem. Pharmacol.*, 1984, **33**, 3235–3239.

31 M. Maiorino, A. Roveri, M. Coassin and F. Ursini, Kinetic mechanism and substrate specificity of glutathione peroxidase activity of ebselen (PZ51), *Biochem. Pharmacol.*, 1988, **37**, 2267–2271.

32 R. S. Glass, F. Farooqui, M. Sabahi and K. W. Ehler, Formation of thiocarbonyl compounds in the reaction of Ebselen oxide with thiols, *J. Org. Chem.*, 1989, **54**, 1092–1097.

33 G. R. Haenen, B. M. de Rooij, N. P. Vermeulen and A. Bast, Mechanism of the reaction of ebselen with endogenous thiols: dihydrolipoate is a better cofactor than glutathione in the peroxidase activity of ebselen, *Mol. Pharmacol.*, 1990, **37**, 412–422.

34 J. K. Pearson and R. J. Boyd, Modeling the Reduction of Hydrogen Peroxide by Glutathione Peroxidase Mimics, *J. Phys. Chem. A*, 2006, **110**, 8979–8985.

35 J. K. Pearson and R. J. Boyd, Density functional theory study of the reaction mechanism and energetics of the reduction of hydrogen peroxide by ebselen, ebselen diselenide, and ebselen selenol, *J. Phys. Chem. A*, 2007, **111**, 3152–3160.

36 K. Forchhammer, W. Leinfelder and A. Böck, Identification of a novel translation factor necessary for the incorporation of selenocysteine into protein, *Nature*, 1989, **342**, 453–456.

37 J. Heider, C. Baron and A. Böck, Coding from a distance: dissection of the mRNA determinants required for the incorporation of selenocysteine into protein, *EMBO J.*, 1992, **11**, 3759–3766.

38 R. E. Huber and R. S. Criddle, Comparison of the chemical properties of selenocysteine and selenocystine with their sulfur analogs, *Arch. Biochem. Biophys.*, 1967, **122**, 164–173.

39 R. J. Hondal and E. L. Ruggles, Differing views of the role of selenium in thioredoxin reductase, *Amino Acids*, 2011, **41**, 73–89.

40 S. M. Kanzok, Substitution of the Thioredoxin System for Glutathione Reductase in Drosophila melanogaster, *Science*, 2001, **291**, 643–646.

41 H. J. Reich and R. J. Hondal, Why Nature Chose Selenium, *ACS Chem. Biol.*, 2016, **11**, 821–841.

42 M. J. Maroney and R. J. Hondal, Selenium versus sulfur: reversibility of chemical reactions and resistance to permanent oxidation in proteins and nucleic acids, *Free Radical Biol. Med.*, DOI: 10.1016/j.freeradbiomed.2018.03.035.

43 G. Ribaudo, M. Bellanda, I. Menegazzo, L. P. Wolters, M. Bortoli, G. Ferrer-Sueta, G. Zagotto and L. Orian, Mechanistic insight into the oxidation of organic phenylselenides by H_2O_2, *Chem. – Eur. J.*, 2017, **23**, 2405–2422.

44 S. Mao, Z. Dong, J. Liu, X. Li, X. Liu, G. Luo and J. Shen, Semisynthetic tellurosubtilisin with glutathione peroxidase activity, *J. Am. Chem. Soc.*, 2005, **127**, 11588–11589.

45 X. Liu, L. A. Silks, C. Liu, M. Ollivault-Shiflett, X. Huang, J. Li, G. Luo, Y. M. Hou, J. Liu and J. Shen, Incorporation of tellurocysteine into glutathione transferase generates high glutathione peroxidase efficiency, *Angew. Chem., Int. Ed.*, 2009, **48**, 2020–2023.

46 E. R. T. Tiekink, Therapeutic potential of selenium and tellurium compounds: opportunities yet unrealised, *Dalton Trans.*, 2012, **41**, 6390.

47 D. F. Meinerz, J. Allebrandt, D. O. Mariano, E. P. Waczuk, F. A. Soares, W. Hassan and J. B. T. Rocha, Differential genotoxicity of diphenyl diselenide $(PhSe)_2$ and diphenyl ditelluride $(PhTe)_2$, *PeerJ*, 2014, **2**, e290.

48 F. Zaccaria, L. P. Wolters, C. Fonseca Guerra and L. Orian, Insights on selenium and tellurium diaryldichalcogenides: a benchmark DFT study, *J. Comput. Chem.*, 2016, **37**, 1672–1680.

49 S. Antony and C. A. Bayse, Modeling the mechanism of the glutathione peroxidase mimic ebselen, *Inorg. Chem.*, 2011, **50**, 12075–12084.

50 G. S. Heverly-Coulson, R. J. Boyd, O. Mó and M. Yáñez, Revealing unexpected mechanisms for nucleophilic attack on S–S and Se–Se bridges, *Chem. – Eur. J.*, 2013, **19**, 3629–3638.

51 E. J. Baerends, D. E. Ellis and P. Ros, Self-consistent molecular Hartree-Fock-Slater calculations I. The computational procedure, *Chem. Phys.*, 1973, **2**, 41–51.

52 G. te Velde, F. M. Bickelhaupt, E. J. Baerends, C. Fonseca Guerra, S. J. A. van Gisbergen, J. G. Snijders and T. Ziegler, Chemistry with ADF, *J. Comput. Chem.*, 2001, **22**, 931–967.

53 C. Fonseca Guerra, J. G. Snijders, G. te Velde and E. J. Baerends, Towards an order-N DFT method, *Theor. Chem. Acc.*, 1998, **99**, 391–403.

54 E. J. Baerends, T. Ziegler, A. J. Atkins, J. Autschbach, D. Bashford, A. Bérces, F. M. Bickelhaupt, C. Bo, P. M. Boerritger, L. Cavallo, D. P. Chong, D. V. Chulhai, L. Deng, R. M. Dickson, J. M. Dieterich, D. E. Ellis, M. van Faassen, A. Ghysels, A. Giammona, S. J. A. van Gisbergen, A. W. Götz, S. Gusarov, F. E. Harris, P. van den Hoek, C. R. Jacob, H. Jacobsen, L. Jensen, J. W. Kaminski, G. van Kessel, F. Kootstra, A. Kovalenko, M. Krykunov, E. van Lenthe, D. A. McCormack, A. Michalak, M. Mitoraj, S. M. Morton, J. Neugebauer, V. P. Nicu, L. Noodleman, V. P. Osinga, S. Patchkovskii, M. Pavanello, C. A. Peeples, P. H. T. Philipsen, D. Post, C. C. Pye, W. Ravenek, J. I. Rodríguez, P. Ros, R. Rüger, P. R. T. Schipper, H. van Schoot, G. Schreckenbach, J. S. Seldenthuis, M. Seth, J. G. Snijders, S. Miquel, M. Swart, D. Swerhone, G. te Velde, P. Vernooijs, L. Versluis, L. Visscher, O. Visser, F. Wang, T. A. Wesolowski, E. M. van Wezenbeek, G. Wiesenekker, S. K. Wolff, T. K. Woo and A. L. Yakovlev, *ADF2016*, SCM, Theoretical Chemistry, Vrije Universiteit Amsterdam, Amsterdam, The Netherlands, 2016.

55 R. van Leeuwen, E. van Lenthe, E. J. Baerends and J. G. Snijders, Exact Solutions of Regular Approximate Relativistic Wave Equations for Hydrogen-Like Atoms, *J. Chem. Phys.*, 1994, **101**, 1272–1281.

56 N. C. Handy and A. J. Cohen, Left-right correlation energy, *Mol. Phys.*, 2001, **99**, 403–412.

57 C. Lee, W. Yang and R. G. Parr, Development of the Colle-Salvetti correlation-energy formula into a functional of the electron density, *Phys. Rev. B: Condens. Matter Mater. Phys.*, 1988, **37**, 785–789.

58 B. G. Johnson, P. M. W. Gill and J. A. Pople, The Performance of a Family of Density Functional Methods, *J. Chem. Phys.*, 1993, **98**, 5612–5626.

59 T. V. Russo, R. L. Martin and P. J. Hay, Density Functional Calculations On First-Row Transition Metals, *J. Chem. Phys.*, 1994, **101**, 7729–7737.

60 A. D. Becke, Density-functional exchange-energy approximation with correct asymptotic behavior, *Phys. Rev. A: At., Mol., Opt. Phys.*, 1988, **38**, 3098–3100.

61 S. Grimme, S. Ehrlich and L. Goerigk, Effect of the damping function in dispersion corrected density functional theory, *J. Comput. Chem.*, 2011, **32**, 1456–1465.

62 S. M. Bachrach and D. C. Mulhearn, Nucleophilic substitution at sulfur: S_N2 or addition–elimination?, *J. Phys. Chem.*, 1996, **100**, 3535–3540.

63 D. C. Mulhearn and S. M. Bachrach, Selective nucleophilic attack of trisulfides. An *ab initio* study, *J. Am. Chem. Soc.*, 1996, **118**, 9415–9421.

64 S. M. Bachrach and B. D. Gailbreath, Theoretical study of nucleophilic substitution at two-coordinate sulfur, *J. Org. Chem.*, 2001, **66**, 2005–2010.

65 S. M. Bachrach, J. M. Hayes, T. Dao and J. L. Mynar, Density functional theory gas- and solution-phase study of nucleophilic substitution at di- and trisulfides, *Theor. Chem. Acc.*, 2002, **107**, 266–271.

66 S. M. Bachrach and A. C. Chamberlin, Theoretical study of nucleophilic substitution at the disulfide bridge of cyclo-L-cystine, *J. Org. Chem.*, 2003, **68**, 4743–4747.

67 T. van Der Wijst, C. Fonseca Guerra, M. Swart, F. M. Bickelhaupt and B. Lippert, A ditopic ion-pair receptor based on stacked nucleobase quartes, *Angew. Chem., Int. Ed.*, 2009, **48**, 3285–3287.

68 C. Fonseca Guerra, T. van der Wijst, J. Poater, M. Swart and F. M. Bickelhaupt, Adenine versus guanine quartets in aqueous solution: dispersion-corrected DFT study on the differences in π-stacking and hydrogen-bonding behavior, *Theor. Chem. Acc.*, 2010, **125**, 245–252.

69 F. M. Bickelhaupt and K. N. Houk, Analyzing Reaction Rates with the Distortion/Interaction-Activation Strain Model, *Angew. Chem., Int. Ed.*, 2017, **56**, 10070–10086.

70 W. J. van Zeist, Y. Ren and F. M. Bickelhaupt, Halogen versus halide electronic structure, *Sci. China: Chem.*, 2010, **53**, 210–215.

71 I. Fernández and F. M. Bickelhaupt, The activation strain model and molecular orbital theory: understanding and designing chemical reactions, *Chem. Soc. Rev.*, 2014, **43**, 4953.

72 L. P. Wolters and F. M. Bickelhaupt, The activation strain model and molecular orbital theory, *Wiley Interdiscip. Rev.: Comput. Mol. Sci.*, 2015, **5**, 324–343.
73 F. M. Bickelhaupt and E. J. Baerends, in *Reviews in Computational Chemistry*, ed. K. B. Lipkovitz and D. B. Boyd, Wiley-VCH, New York, 2000, vol. 15, pp. 1–86.
74 W. J. van Zeist, C. Fonseca Guerra and F. M. Bickelhaupt, PyFrag—Streamlining your reaction path analysis, *J. Comput. Chem.*, 2007, **28**, 73–86.
75 M. Torsello, A. C. Pimenta, L. P. Wolters, I. S. Moreira, L. Orian and A. Polimeno, General AMBER Force Field Parameters for Diphenyl Diselenides and Diphenyl Ditellurides, *J. Phys. Chem. A*, 2016, **120**, 4389–4400.
76 F. M. Bickelhaupt, M. Solà and P. von Ragué Schleyer, Theoretical investigation of the relative stabilities of XSSX and X_2SS isomers (X = F, Cl, H, and CH_3), *J. Comput. Chem.*, 1995, **16**, 465–477.
77 M. El-Hamdi, J. Poater, F. M. Bickelhaupt and M. Solà, X_2Y_2 Isomers: Tuning Structure and Relative Stability through Electronegativity Differences (X = H, Li, Na, F, Cl, Br, I; Y = O, S, Se, Te), *Inorg. Chem.*, 2013, **52**, 2458–2465.
78 J. Młochowski and H. Wójtowicz-Młochowska, Developments in Synthetic Application of Selenium(IV) Oxide and Organoselenium Compounds as Oxygen Donors and Oxygen-Transfer Agents, *Molecules*, 2015, **20**, 10205–10243.